Novel 1-D Organic–Inorganic Polyoxometalate Hybrids Constructed from Heteropolymolybdate Units and Copper–Aminoacid Complexes

Jun-Wei Zhao,*[,†,‡] Jing-Li Zhang,[†] Yan-Zhou Li,[†] Jing Cao,[†] and Li-Juan Chen*[,†]

[†]Institute of Molecular and Crystal Engineering, Henan Key Laboratory of Polyoxometalate Chemistry, College of Chemistry and Chemical Engineering, Henan University, Kaifeng, Henan 475004, People's Republic of China

[‡]State Key Laboratory of Structural Chemistry, Fujian Institute of Research on the Structure of Matter, Chinese Academy of Sciences, Fuzhou, Fujian 350002, People's Republic of China

Supporting Information

Scheme S1. The structure of L-arginine.

Figure S1. IR spectra of **1**, **2**, $(NH_4)_6Mo_7O_{24}\cdot 4H_2O$ (Mo_7) and L-arginine (arg).

Figure S2. The 3-D supramolecular structure of **2** via hydrogen-bonding interactions between arg groups and POAs / lattice waters.

Figure S3. The TG curves of **1** and **2**.

Figure S4. Cyclic voltammogram of $(NH_4)_6Mo_7O_{24}\cdot 4H_2O$ in 1 mol·L^{-1} H_2SO_4 aqueous solution. Scan rate: 50 mV s^{-1}.

Figure S5. Cyclic voltammograms of $(NH_4)_6Mo_7O_{24}\cdot 4H_2O$ in 1 mol·L^{-1} H_2SO_4 aqueous solution containing various concentrations (a 1×10^{-3}, b 3×10^{-3}, c 5×10^{-3}, d 7×10^{-3}, e 9×10^{-3}, f 1.1×10^{-2} mol·L^{-1}) of $NaNO_2$. Scan rate: 50 mV s^{-1}.

Figure S6. Cyclic voltammograms of $(NH_4)_6Mo_7O_{24}\cdot 4H_2O$ in 1 mol·L^{-1} H_2SO_4 aqueous solution containing various concentrations (a 1×10^{-3}, b 3×10^{-3}, c 5×10^{-3}, d 7×10^{-3}, e 9×10^{-3} mol·L^{-1}) of $NaBrO_3$. Scan rate: 50 mV s^{-1}.

Table S1. The Hydrogen bonds for **1** (Å and °)

Table S2. The Hydrogen bonds for **2** (Å and °)

Thermal Properties

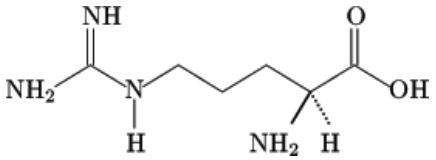

Scheme S1. The structure of L-arginine.

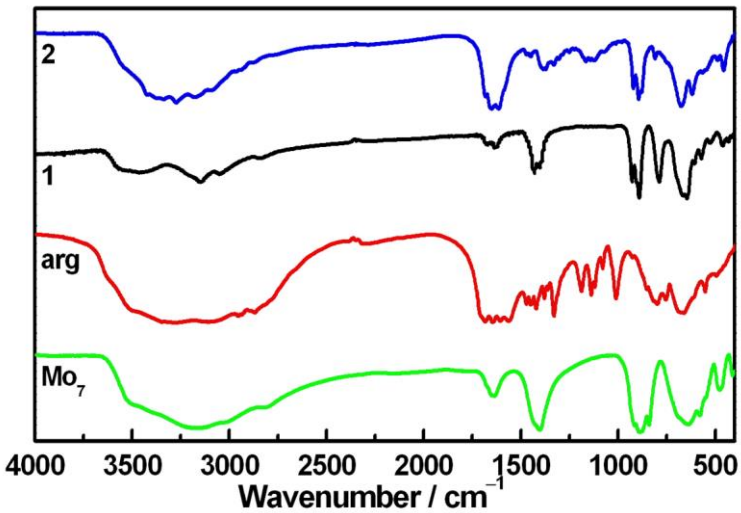

Figure S1. IR spectra of **1**, **2**, $(NH_4)_6Mo_7O_{24}\cdot 4H_2O$ (Mo_7) and L-arginine (arg).

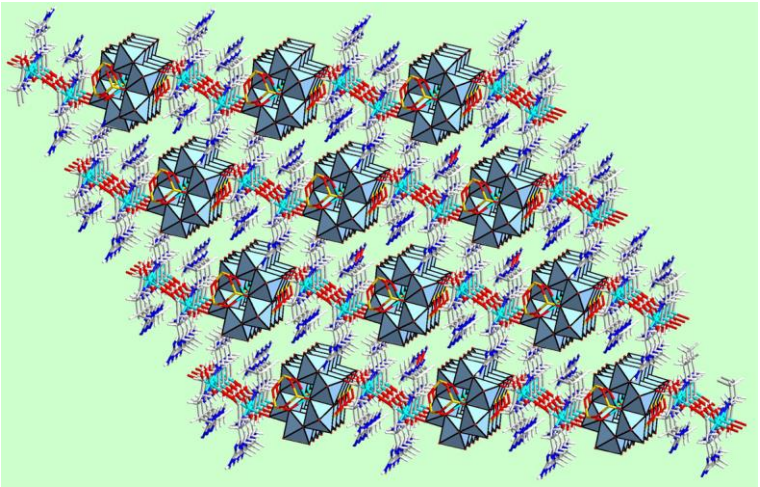

Figure S2. The 3-D supramolecular structure of **2** via hydrogen-bonding interactions between arg groups and POAs / lattice waters.

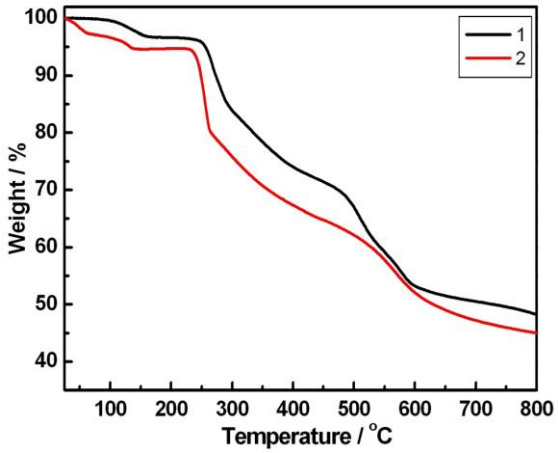

Figure S3. The TG curves of **1** and **2**.

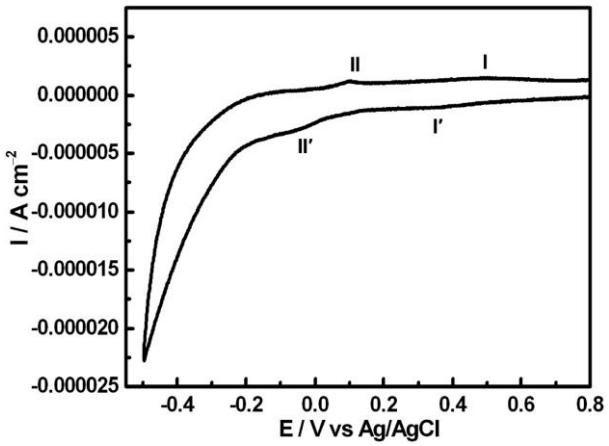

Figure S4. Cyclic voltammogram of $(NH_4)_6Mo_7O_{24}{\cdot}4H_2O$ in 1 mol·L^{-1} H_2SO_4 aqueous solution. Scan rate: 50 mV s^{-1}.

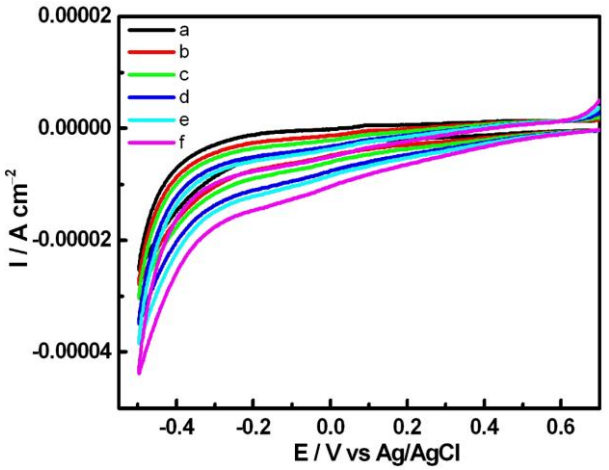

Figure S5. Cyclic voltammograms of $(NH_4)_6Mo_7O_{24}{\cdot}4H_2O$ in 1 mol·L^{-1} H_2SO_4 aqueous solution containing various concentrations (a 1×10^{-3}, b 3×10^{-3}, c 5×10^{-3}, d 7×10^{-3}, e 9×10^{-3}, f 1.1×10^{-2} mol·L^{-1}) of $NaNO_2$. Scan rate: 50 mV s^{-1}.

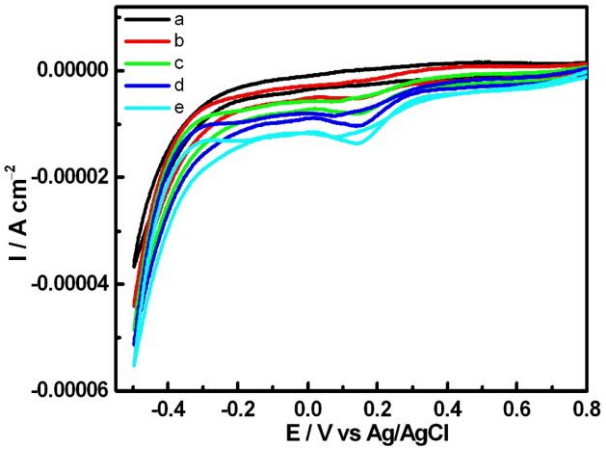

Figure S6. Cyclic voltammograms of $(NH_4)_6Mo_7O_{24}\cdot 4H_2O$ in 1 mol·L^{-1} H_2SO_4 aqueous solution containing various concentrations (a 1 × 10^{-3}, b 3 × 10^{-3}, c 5 × 10^{-3}, d 7 × 10^{-3}, e 9 × 10^{-3} mol·L^{-1}) of $NaBrO_3$. Scan rate: 50 mV s^{-1}.

Table S1. The Hydrogen bonds for 1 (Å and °)

D–H···A	d(D–H)	d(H···A)	d(D···A)	<(DHA)
N(1)–H(1B)···N(8)#2	0.90	2.52	3.379(4)	160.9
N(2)–H(2B)···O(19)#3	0.86	2.01	2.8682(12)	175.0
N(3)–H(3C)···O(5)#4	0.86	2.16	2.955(8)	152.8
N(3)–H(3D)···O(11)#5	0.86	2.32	3.128(8)	156.9
N(3)–H(3D)···O(12)#5	0.86	2.46	3.069(9)	128.2
N(4)–H(4C)···O(18)#3	0.75	2.12	2.844(8)	162.3
N(5)–H(5A)···O(1W')#6	0.90	2.55	3.15(2)	124.6
N(5)–H(5A)···O(17)#7	0.90	2.65	3.114(4)	113.2
N(5)–H(5B)···O(8)	0.90	2.23	3.060(7)	153.4
N(6)–H(6A)···O(17)#8	0.86	1.99	2.8438(12)	172.6
N(7)–H(7B)···O(2W')#9	0.75	2.27	2.94(2)	149.0
N(7)–H(7B)···O(2W)#9	0.75	2.51	3.19(3)	151.3
N(8)–H(8A)···O(1W')#9	0.86	2.13	2.86(2)	143.1
N(8)–H(8A)···O(1)#9	0.86	2.50	3.096(9)	127.4
N(8)–H(8B)···O(16)#8	0.86	2.13	2.976(8)	165.8

Symmetry transformations used to generate equivalent atoms: #1 –*x*+1, –*y*+1, –*z*; #2 –*x*, –*y*+2, –*z*+1; #3 *x*+1, *y*, *z*; #4 –*x*+1, –*y*+1, –*z*+1; #5 *x*+1, *y*, *z*+1; #6 *x*, *y*+1, *z*; #7 –*x*+1, –*y*+2, –*z*+1; #8 *x*–1, *y*, *z*; #9 *x*–1, *y*+1, *z*

Table S2. The Hydrogen bonds for 2 (Å and °)

D–H···A	d(D–H)	d(H···A)	d(D···A)	<(DHA)
O(1)–H(1A)···O(4W)#3	0.82	2.11	2.816(9)	144.7
O(4)–H(4A)···N(8)#4	0.82	2.13	2.721(6)	128.9
O(6)–H(6A)···N(8)#5	0.82	1.99	2.784(7)	161.3
N(1)–H(1B)···O(16)#6	0.86	2.62	3.317(7)	138.6
N(1)–H(1C)···O(10)#7	0.86	2.06	2.839(6)	149.4
N(2)–H(2C)···O(12)#7	0.75	2.27	3.016(6)	170.8
N(3)–H(3C)···O(16)#6	0.86	2.02	2.860(6)	166.9
N(4)–H(4B)···O(15)#6	0.90	2.18	2.977(7)	146.7
N(4)–H(4C)···N(7)#3	0.90	2.45	3.296(10)	155.8
N(5)–H(5A)···O(17)#1	0.90	1.99	2.881(6)	170.0

N(5)–H(5B)···O(15)#6	0.90	2.19	2.977(5)	145.2
N(5)–H(5B)···O(12)#6	0.90	2.60	3.167(6)	122.1
N(6)–H(6B)···O(9)#3	0.86	2.33	3.033(6)	138.8
N(6)–H(6B)···O(13)#6	0.86	2.40	3.074(6)	135.6
N(7)–H(7A)···O(9)#3	0.86	2.20	2.895(6)	137.3
N(7)–H(7A)···O(8)#3	0.86	2.48	3.242(6)	148.1
N(7)–H(7B)···O(5)#8	0.86	2.03	2.892(7)	175.4
N(8)–H(8B)···O(4)#4	0.75	2.06	2.721(6)	147.4
N(9)–H(9A)···O(11)	0.90	2.09	2.990(6)	175.1
N(9)–H(9B)···O(2)	0.90	2.19	3.073(7)	167.0
N(10)–H(10C)···O(7)	0.86	2.27	3.044(6)	149.9
N(11)–H(11C)···O(7)	0.86	2.41	3.159(6)	145.4
N(11)–H(11D)···O(18)#9	0.86	2.10	2.960(6)	175.1
N(12)–H(12A)···O(14)#9	0.75	2.11	2.835(6)	161.6

Symmetry transformations used to generate equivalent atoms: #1 –*x*, –*y*+2, –*z*+1; #2 –*x*, –*y*+2, –*z*; #3 –*x*–1, –*y*+2, –z+1; #4 –*x*–1, –*y*+1, –*z*+1; #5 *x*+1, y, *z*–1; #6 *x*–1, *y*, *z*; #7 *x*–1, *y*+1, *z*; #8 *x*–1, *y*, *z*+1; #9 *x*, *y*–1, *z*

Thermal Properties

The thermal stability of **1** and **2** has been investigated on crystalline samples under air atmosphere with a heating rate of 10 °C/min in the temperature range of 25–800 °C (Figure S3). The TG curve of **1** shows three steps of weight loss. The first weight loss of 2.79% from 25 to 143 °C is ascribed to the release of four lattice water molecules (calcd. 2.92%). The second weight loss of 28.95% from 143 to 486 °C corresponds to the removal of four arg ligands (calcd. 28.27%). Then, the third weight loss of 20.18% up to 800 °C is assigned to the sublimation of part As_2O_3 resulting from the decomposition of the POA skeleton of **1**.[1] The TG curve of **2** exhibits two-step weight loss, giving a total loss of 48.68% (calcd.48.20%). The first weight loss of 5.43% from 25 to 139 °C is assigned to the liberation of eight lattice water molecules (calcd. 5.84%). The second weight loss of 43.25% from 139 to 800 °C corresponds to the removal of arg (calcd. 42.36%). The observed experimental values are in good agreement with the elemental analyses and the results of sing-crystal X-ray structural analyses.

(1) Su, F. Y.; Zhou, B. B.; Zhao, Z. F.; Su, Z. H.; Zhu, C. C. *Cryst. Res. Technol.* **2009**, *44*, 447.